

ABSTRACT

The 34-nucleotide *trans*-activator (TA) element within RNA-2 of *Red clover necrotic mosaic virus* is predicted to fold into a simple stem-loop structure. The 8-nucleotide TA loop base pairs with a complementary 8-nucleotide element (the TA binding sequence or TABS) within the capsid protein (CP) subgenomic RNA (sgRNA) promoter on RNA-1. This interaction *trans*-activates CP sgRNA synthesis from RNA-1. Mutations within the 8-nucleotide TA loop indicated that a minimum interaction of 6 base pairs, comprising the contiguous GC stretch, is required for efficient *trans*-activation. TA stem mutations revealed that stem maintenance is critical for TA activity. The TA element is active when expressed from viral RNA constructs but not from transient DNA expression vectors. The TA-TABS interaction occurs with the positive strand RNAs. These experiments genetically establish that the stem-loop structure of the TA and high levels of expression/accumulation of both TA and TABS RNAs are required for efficient *trans*-activation.

Keywords: RCNMV; *Dianthovirus*; *trans*-activator; subgenomic RNA; transcription regulation; RNA-RNA interactions; *Tomato bushy stunt virus*; DI-RNA

INTRODUCTION

Red clover necrotic mosaic virus (RCNMV) is a member of the *Dianthovirus* genus, *Tombusviridae* family along with *Carnation ringspot virus* (CRSV) and *Sweet clover necrotic mosaic virus* (SCNMV). The RCNMV genome consists of two positive sense, single stranded RNAs of 3.9 and 1.5 kb packaged into 32 nm icosahedral virions (Lommel et al., 1988; Xiong and Lommel, 1989). The larger genomic RNA-1 encodes two open reading frames (ORFs). The 5' proximal ORF, interrupted by a -1 ribosomal frameshifting signal, produces a pre-readthrough 27 kDa protein and an 88 kDa polypeptide which is the viral encoded replicase (Xiong et al., 1993b; Kim and Lommel, 1994, 1998). The second 3' proximal ORF encodes the 37 kDa capsid protein (CP; Fig. 1A) which is required for long distance movement (Xiong et al., 1993a; Vaewhongs and Lommel, 1995). This ORF is expressed *in vivo* from a subgenomic RNA (sgRNA; Zavriev et al., 1996). The smaller RNA-2 is monocistronic and encodes the 35 kDa movement protein (MP) required for cell-to-cell movement (Lommel et al., 1988; Osman and Buck, 1987; Xiong et al., 1993a).

RCNMV RNA-2 is required and must be replicating in the presence of RCNMV RNA-1 to initiate sgRNA synthesis for CP expression (Sit et al., 1998). sgRNA synthesis from RCNMV RNA-1 can also be initiated by the RNA-2 from either CRSV or SCNMV. A 34 nucleotide element within RCNMV RNA-2 is sufficient to *trans*-activate sgRNA synthesis from RNA-1. This minimum *trans*-activator or TA element is predicted to form a stem-loop structure (Fig.1A). The 8 nucleotides comprising the loop are complementary with 8 nucleotides in the RNA-1 subgenomic promoter just 2 nucleotides upstream from the sgRNA transcription start site. A previous mutation study

has genetically established that the TA loop basepairs with this RNA-1 8 nucleotide element termed the *trans*-activator binding site (TABS) within the subgenomic promoter.

To date, this interaction between the two genomic RNAs of RCNMV and those predicted for the two other species comprising the *Dianthovirus* genus are the only *trans*-interactions established to direct sgRNA synthesis. However, there are a growing number of RNA viruses in which a long distance *cis* RNA interaction is required to facilitate sgRNA synthesis. *Cis*-acting interactions have been determined for two taxonomically distinct monopartite plant viruses; *Potato virus X* (PVX; Kim & Hemenway, 1999); and *Tomato bushy stunt virus* (TBSV; Zhang et al., 1999; Choi et al., 2001; Choi and White, 2002). More recently, a *cis* interaction has also been demonstrated for sgRNA (RNA3) synthesis in the bipartite insect virus *Flock house virus* (FHV) from its RNA1 (Lindenbach et al., 2002). Interestingly, FHV RNA3 synthesis is required to *trans*-activate replication of FHV RNA2 (Eckerle and Ball, 2002; Eckerle et al., 2003) which in turn, down regulates RNA3 synthesis (Zhong and Rueckert, 1993). Sequence analysis of the *Cocksfoot mottle virus* (a plant sobemovirus) and its associated defective interfering RNA (DI-RNA) suggest that a 7 nt element representing the terminal loop of a putative simple stem-loop structure can base-pair with a region just upstream from the start site of the single CP sgRNA (S.K. Zavriev, personal communication). This stem-loop is approximately 400 nt downstream from the sgRNA start site on the genomic RNA. Interestingly, the stem-loop sequence is also present in the DI-RNA. Consequently, this interaction has the potential of being a *cis* and or a *trans* interaction.

It has been hypothesized that viral sgRNAs are manufactured by one of three different mechanisms: (i) internal initiation on negative RNA strands, (ii) discontinuous RNA transcription, and (iii) premature transcription termination (Miller & Koev, 2000). Until recently evidence only existed for sgRNA synthesis by the first two mechanisms. More recent data suggests that viruses requiring a *cis* or *trans* RNA interaction near the subgenomic start site actually synthesize sgRNA by a premature termination mechanism (White, 2002). It is possible that a premature termination mechanism is utilized by all viruses in which an RNA-RNA interaction is required for sgRNA synthesis.

In this study we genetically define the extent of the RNA-RNA interaction required to *trans*-activate sgRNA synthesis. We have determined that the stem-loop structure with an 8-nucleotide loop is required for *trans*-activation. Furthermore, the TATABS interaction requires a minimum of six sequential GC base pairs for efficient *trans*-activation. Expression and accumulation levels of the TA from strong plant promoters are insufficient to initiate the RNA-RNA interaction required for *trans*-activation. However, expression of the TA from a high copy DI-RNA does lead to *trans*-activation. Thus, large concentrations of the two RNA components are required to shift the equilibrium towards an RNA-RNA interaction.

RESULTS

Co-variation analysis reveals a minimum 7 base interaction between the TATABS

Based on the interchangeability of RNA-2's among the three *Dianthovirus* species for *trans*-activation (Sit et al., 1998), a phylogenetic analysis of the various

RNA-1 TABS was performed. This analysis revealed a strict conservation of 6-nucleotides in the RNA-1 subgenomic promoter capable of pairing with the RNA-2 TA loop (Fig. 1A). Since the TA loop sequence is identical for all three dianthoviruses, it was hypothesized that the minimal TA/TABS interaction required 6 base pairs. The initial RCNMV RNA-2 TA element study (Sit et al., 1998) assayed the *trans*-activation property of a compensatory mutation between the TA and the TABS. Since the RNA-1 TABS was located within the p88 ORF, a single mutant, designated R1sGFP-M (Fig. 1B), was generated with 3 nucleotide changes designed to minimally alter the amino acid sequence of the replicase. This RNA-1 mutant was complemented by an RNA-2 TA loop mutant (expressed from the TBSV vector, pHST2) with three compensatory nucleotide changes (TA MUT, Fig. 2) restoring full base-pairing potential with the altered TABS and reconstituting wild-type levels of *trans*-activation (Sit et al., 1998).

In this study, all single and pair-wise mutations from the original triple residue mutant (TA MUT) were synthesized in the TA loop (mutants M1-M6, Fig. 2) and assayed for their ability to *trans*-activate sGFP expression from both wild-type R1sGFP and the TABS mutant R1SGFP-M on *Nicotiana benthamiana* plants. Only the single nucleotide change mutant M1, containing 7 potential base pairs with R1sGFP, elicited sGFP production at wild-type levels from R1sGFP (Fig. 3B). Although mutants M2 and M3 could conceivably form 7 base pairs with R1sGFP, sGFP expression was less than 10% of wild-type for mutant M3 (compare Figs. 3A & C) and not detectable for mutant M2. Additionally, mutants M4-M6 each contain 6 potential base pairs with R1sGFP but only mutant M5 induced limited sGFP expression from R1sGFP (Fig. 2 & Fig. 3D,

mutant M6). We conclude that 7 base pairs between the TA/TABS are required for efficient *trans*-activation of R1sGFP.

When R1sGFP-M was assayed with M1-M6 mutant transcripts, only mutants M2 and M6 could induce sGFP production albeit at less than 10% with respect to TA MUT (Fig. 2) despite only 6 potential base pairs for mutant M2 compared to 7 base pairs for mutant M6. This result for mutant M6 was surprising since it was expected to induce sGFP expression from R1sGFP-M at levels comparable to TA MUT because the same GC base pairs between mutant M1 and R1sGFP resulted in wild-type levels of sGFP synthesis. A result similar to mutant M3 with R1sGFP was also expected for mutant M4 with R1sGFP-M since the same potential base pairs could be formed in both cases, but this was not observed (Fig. 2). Only the comparable pairings of mutants M2 and M5 with R1sGFP and R1sGFP-M produced the expected co-variation results.

A minimum of 6 sequential GC base-pairs between RNA-1 TABS and RNA-2 TA is required for efficient *trans*-activation

The co-variation analysis was limited to examining 6-7 base pairs as the minimum complementarity between the TA/TABS elements. To determine if an interaction consisting of fewer than 6 base pairs was viable, mutants consisting of sequential nucleotide changes from 5' to 3' were introduced into the RNA-2 TA loop sequence. The nucleotide changes were designed such that the highly conserved 6 GC base pairs between the TA/TABS would be the least affected. These mutants (M14-M18, Fig. 4) reduced the number of potential base pairs from 6 for mutants M14 and M15 down to 3 for mutant M18. Mutants M14 and M15 both have the potential to form 6

base pairs with the TABS but mutant M14 was designed to make the loop region smaller by introducing the potential for an intramolecular GC base pair between the first and last nucleotides of the TA loop (Fig. 4). This difference between mutants M14 and M15 can be seen in the greater accumulation of sGFP from mutant M15 (near wild-type) compared to mutant M14 (~25% of wild-type). Co-inoculation of mutant M16 with R1sGFP did not lead to detectable sGFP synthesis despite the potential for 5 sequential base pairs (compare to mutants M3 and M5). Mutants M17 and M18 did not induce detectable sGFP production from R1sGFP (Fig. 4). From these results, we conclude that the 6 sequential GC base pairs between the TA/TABS elements are essential and sufficient for efficient *trans*-activation.

The TA/TABS interaction is unstable with non-canonical base pairing

One of the unanswered questions raised in the initial study was whether the RNA-RNA interactions occurred between positive or negative RNA strands since the TA/TABS complementarity exists in both strands. To address this issue, strand specific nucleotide changes were introduced into loop mutants M19-M21 and M27. These mutations converted GC base pairs to non Watson-Crick GU base pairs depending on whether the TA/TABS interaction occurred on the positive (mutants M19-M21) or negative (mutant M27) RNA strands. Mutants M19-M21 introduced 1-3 base pair changes, respectively, while mutant M27 incorporated a single base pair change. Only mutant M19 exhibited detectable *trans*-activating ability (25% of wild-type; see Fig. 4) when co-inoculated with R1sGFP. The lack of detectable sGFP production with mutant M27 combined with the results from mutant M19 suggests that the TA/TABS interaction

takes place between positive RNA strands. However, the lack of sGFP production from co-inoculations with mutants M20 and M21 suggest that the TA/TABS interaction is either weakened or unstable when GC base pairs are exchanged with GU base pairs.

The primary RNA-2 TA stem sequence is not essential as long as stem structure is maintained

The proposed structure of the RNA-2 TA element consists of an 8 nt loop attached to a stem composed of 2 helical regions (H1 & H2) separated by a bulge (Fig. 5). Phylogenetic analysis revealed that only the loop region and the top 3 base pairs of H1 are strictly conserved among the dianthoviruses, all of which can biologically *trans*-complement. However, we have previously shown that a 20 nt element consisting only of the loop and the upper helical region (H1) *trans*-activates but at an attenuated level compared to the full 34 nt element (Sit et al., 1998) suggesting that both helical regions were required for optimal activity.

Mutants M7-M12 introduced mutations into H1 and the bulge of the RNA-2 TA stem without altering the lower helical region (H2). Mutants M7 and M10 were constructed to determine the requirement for the bulge by either removing it completely (mutant M7) or by transposing the orientation of the bulge with respect to the stem (mutant M10; Fig. 5). Both mutations had no appreciable reduction of *trans*-activation levels.

Mutants M8 and M9 were designed to test the effect of changes to the primary sequence of H1 while maintaining both the sequence and helical structure. Mutant M8 was produced by transposing and inverting H1 while mutant M9 was produced by

merely transposing H1. Mutant M8 accumulated wild-type levels of sGFP. Surprisingly, mutant M9 did not exhibit detectable *trans*-activation despite the conservation of base pairing (Fig. 5).

To isolate the base pair(s) in H1 responsible for the loss of *trans*-activation observed in mutant M9, two additional mutants were constructed, mutants M11 and M12, by transposing either the lower or upper 3 base pairs of H1, respectively (Fig. 5). Mutant M11 exhibited wild-type levels of *trans*-activation while mutant M12 produced sGFP at less than 10% of wild-type levels. Therefore, the upper 3 base pairs of H1 are critical for full TA functionality as suggested by the phylogenetic analysis. It was observed after designing and testing mutants M9 and M12 that the neck GU base pair, if unpaired, could lead to 10 potential base pairs between the TA and the TABS (compare Fig. 1A and Fig. 5).

The base pair at the top of H1 is structurally critical for *trans*-activator activity

An *in vitro* model system of the TA/TABS interaction, utilizing short oligoribonucleotides, was devised (Guenther et al., manuscript in review). Computer modeling of NMR data from these experiments revealed that the neck UG base pair at the top of H1 was a critical component of the complex structure. To genetically and biologically corroborate this feature of the model, mutants M13, M22 and M23 were produced. Mutant M13 replaced the UG base pair with the more stable CG base pair to assess if H1 stem stability was important for *trans*-activation. The levels of sGFP induced by mutant M13 did not differ significantly from the wild-type TA. Mutant M22 replaced the wild-type UG base pair with a UA base pair. Mutant M22 also did not affect

sGFP accumulation compared to the wild-type TA (Fig. 5). Mutant M23 transposed the UG base pair to a GU base pair as found in mutants M9 and M12. This resulted in mutant M23 producing sGFP at less than 10% of wild-type TA levels, similar to mutant M12. Thus, the alteration of the non-canonical UG neck base pair appears to be responsible for the dramatic decrease in RNA-2 TA activity for mutants M9 and M12.

RNA-2 TA stem mutations suggest a (+/+)-strand TA/TABS interaction

Since the substitution of GC base pairs with GU base pairs in the TA loop proved inconclusive in determining the nature of the strand interaction between the TA/TABS, alternative mutations were produced by insertion of GU base pairs into the H1 stem of the RNA-2 TA. H1 appears to tolerate primary sequence changes readily since the only base pair critical for full TA function resides atop of H1. Mutants M25 and M26 contained separate, single GC→GU base pair conversions while M24 combined both individual mutations (Fig. 5). Mutants M28 and M29 contain separate, individual GC→AC changes (which lead to potential GU base pairs in the negative strands) while mutant M30 combines both individual mutations (Fig. 5). Mutants M25 and M26 induced sGFP production at 25% and 50% of wild-type TA level, respectively. When the mutations were combined in mutant M24, *trans*-activation diminished to less than 10% of wild-type TA levels. Despite the reduction in TA activity, mutants M24-26 were all able to induce detectable levels of sGFP synthesis. In contrast, mutants M28-30 (which generate UG base pairs in the negative strand) did not exhibit sGFP synthesis when co-inoculated with R1sGFP. Taken together, these results suggest that the TA/TABS interaction occurs between positive RNA strands since the GU base pairs of mutants

M24-26 would exist as non-paired AC residues in the negative strand, sufficiently disrupting the stem structure to completely prevent detectable *trans*-activation.

Expression of the TA from DNA-based plant expression vectors is not sufficient for *trans*-activation

To unequivocally determine which strand the TA/TABS interaction occurs in, the RCNMV RNA-2 MP ORF (which contains the TA element) was expressed in both positive and negative sense orientations from the DNA-based plant expression vectors pRTL2 (Carrington et al., 1990) and pE1578 (Ni et al., 1995). Since transcription occurs from only one strand of the encoded DNA sequence, it was hypothesized that only the construct expressing the correct strand would *trans*-activate sGFP synthesis from co-bombarded R1sGFP transcripts. Co-bombardment of the RNA-2 TA element expressed from either the dual 35S promoter containing plasmid pRTL2 or the super promoter containing plasmid pE1578 with R1sGFP transcripts in both instances failed to express sGFP to detectable levels (see Table 1). The positive control plasmids encoding sGFP did express sGFP when bombarded alone as did transcripts of R1sGFP co-bombarded with RCNMV RNA-2.

The RNA-2 TA element is functional when expressed from a high copy TBSV DI-RNA

The lack of *trans*-activation when the TA is expressed from DNA-based transient expression vectors may be related to the level of RNA transcription generated by DNA promoters. In earlier studies, the TA element was expressed as part of a TBSV sgRNA

that is similar in size to RCNMV RNA-2 and is expressed and accumulates at high levels. To determine if the RNA size and copy number are critical for TA activity, the RNA-2 TA element was cloned and expressed from a TBSV DI-RNA (DI-72SXP; Ray and White, 1999) that was only 618 nt in length. Co-inoculation of the DI-TA construct with R1sGFP and either the pHST2 vector or wild-type TBSV as a helper virus, led to the production of sGFP from R1sGFP at levels comparable to that induced by wild-type RNA-2 (Fig. 6). Co-inoculations of DI-72SXP (without the TA insert) with R1sGFP and pHST2 as a helper virus did not lead to production of detectable sGFP on either wild-type *N. benthamiana* or RCNMV MP+ transgenic *N. benthamiana* (data not shown).

Discussion

The RNA-2 TA element is essential for the initiation of CP sgRNA synthesis from RNA-1 in RCNMV. This element is conserved among the Dianthoviruses and is assumed to function in the same manner for both CRSV and SCNMV since the genomic RNA-2's are all interchangeable for infectivity (Okuno et al., 1983; Sit, T.L., Haikal, P.R. & Lommel, S.A., unpublished). This fact also reveals the existence of a conserved intermolecular communication mechanism between the two genomic RNAs which is involved in the regulation of gene expression. The location of the TA element within the MP ORF on RNA-2 illustrates the compact nature of the RCNMV genome where RNA sequences can perform multiple functions. In the mutagenesis studies presented, we have expressed the TA element from a TBSV vector, pHST2, to isolate its role in initiating sgRNA synthesis from other potential functions during the viral replication

cycle. Since the TBSV sgRNA promoters are not influenced by RCNMV-specific sequence elements, the level of TA element synthesis should be consistent regardless the mutation. This would not have been the case if the mutations were made directly in RCNMV RNA-2 where accumulation levels may have been affected by changes to the primary RNA-2 sequence. One drawback of this approach is that TA expression and accumulation is not dependent on RCNMV RNA-1 and thus may mask subtleties in the dynamics of the sgRNA regulation mechanism such as the intracellular localization of the TA element or the exact timing of the *trans*-activation event during the replication process. Additionally, since the pHST2-TA mutant constructs are capable of independent replication, many foci of infection contained only the TA mutant construct without RCNMV RNA-1 which complicates interpretation of the mutant's ability to *trans*-activate. Furthermore, we cannot examine the potential effects a mutant would have on a negative feedback regulation mechanism which would curtail sgRNA synthesis by, for example, encapsidation of genomic RNA-2. This feedback mechanism has been well documented for FHV RNA3 and the negative effect of genomic RNA2 accumulation on the levels of RNA3 (Zhong and Rueckert; Eckerle and Ball, 2002).

The original TA study assumed a stem loop structure for the TA element based on predictions from the Mfold server (Zuker, 2003). This structure (depicted in Figs. 1A and 5) consists of an 8 nt loop atop a stem consisting of two helical regions (H1 and H2) that are separated by a 5 nt bulge. A 20 nt reduced version of the TA element (containing the loop plus H1 but lacking H2) was still capable of initiating *trans*-activation but at severely reduced levels (Sit et al., 1998). This suggested the possibility of steric hindrance or element presentation playing a role in the ability of the TA to bind

to the TABS. Furthermore, the isolated loop sequence was incapable of *trans*-activation suggesting that intramolecular base pairing in the stem was strictly required. For this reason, mutations were confined to the loop, H1 (with maintenance of base-pairing) and bulge regions of the 34 nt TA element so that subtle differences in expression levels could be easily observed.

The results of the present study reinforce the requirement for a specific RNA-RNA interaction between the TA and TABS elements for successful *trans*-activation. Based on the compensatory loop mutation experiments involving mutants M1-M6, a minimum 7 nt interaction is required for wild-type activity (see Fig. 2, R1sGFP + mutant M1). However, this conclusion is complicated by the results for R1sGFP-M + mutant M6 where a similar positioned mutation leads to sGFP expression at only 10% of TA MUT induced levels. This may be due to the formation of an alternate simple hairpin structure based on the self-complementarity of the mutant M6 loop sequence (Fig. 2) which would inhibit TA/TABS interactions. The reduced level of expression induced by mutant M3 with R1sGFP reveals the further requirement of the 6 contiguous GC loop nucleotides for optimal activity. This is in agreement with the phylogenetic conservation of 6 GC base pairs between the TA/TABS of the dianthoviruses (Fig. 1A). The TA/TABS interaction must also include a stretch of at least 5 contiguous base pairs since mutants M2, M4 and M6 did not induce sGFP expression while mutant M5 did when co-inoculated with R1sGFP. Similar conclusions can be made for mutants M1, M3 and M5 with respect to R1sGFP-M. One unexpected result was the lack of sGFP expression with R1sGFP-M and mutant M4 which was expected to behave much like R1sGFP with

mutant M3. This may have been due to subtle differences in the stability of the M3 versus M4 loop sequences when bound to their respective TABS.

Results obtained with loop mutants M14-M18 further reinforce the requirement of 6 GC base pairs in an open loop for the TA/TABS interaction. Although mutant M14 has the potential to form 7 base pairs between the TA/TABS (much like mutant M1) sGFP induction was markedly reduced. This may be due to a smaller TA loop structure which would diminish the TA/TABS interaction much like mutant M6 and its potential to change the loop to a hairpin. The lack of sGFP induction by mutant M16 was unexpected since mutants M3 and M5, which can potentially form 5 base pairs, were still able to generate limited expression, albeit less than 10% of wild type. This may be explained by the findings of the *in vitro* oligoribonucleotide studies where the most stable interacting pair of oligoribonucleotides excluded the terminal C nucleotide of the TA loop as found in mutants M3 and M5 (Guenther et al., manuscript in review).

The bulge and H1 stem of the TA element were probed with mutants M7-M12. The bulge does not appear to be essential since translocation (mutant M10) or removal (mutant M7) did not affect the ability to *trans*-activate. However, the bulge may play other roles in the RCNMV replication cycle which are beyond the scope of these experiments. The presence of the bulge may also reflect the need to conserve the underlying primary sequence for a functional MP. The H1 stem sequence also appears to be amenable to alteration as long as the base pairing is maintained since mutant M8 transposed and inverted the H1 sequence. However, mutant M9 showed a loss of sGFP induction after the transposition of H1 base pairs. Mutants M11 and M12 narrowed the responsible region to the upper 3 base pairs of H1. The potential for 10 base pairs

between the TA/TABS for mutants M9 and M12 exists if the GU base pair at the top of H1 were unpaired. This potential increase in base pairing is unlikely to be the cause of reduced sGFP levels since the induction of sGFP in this assay is not dependent on full-length viral replication which would be diminished as a result of the enhanced stability of the TA/TABS complex. A more likely scenario could be deduced from the results of mutants M13, M22 and M23 where subtle changes were applied solely to the closing base pair at the top of H1. Mutant M23 displays the same reduced sGFP accumulation phenotype as mutants M9 and M12. Thus, the neck base pair appears to be critical for efficient *trans*-activation. It appears there is flexibility with regard to the particular residues involved as long as there is maintenance of the positional pyrimidine/purine combination. This may reflect a structural requirement for this particular base pairing to allow formation of the TA/TABS complex.

To determine whether the + or - strand of the RNAs interacted for TA/TABS complex formation, several strategies were employed. The most straightforward approach appeared initially to be co-bombardment of R1sGFP with DNA expression vectors that would express either the positive or the negative stranded version of the TA element. Both of the plant expression vectors were chosen based on their high level of reporter gene expression. This proved to be an experimental limitation since the transcriptional activity of the promoters was not directly correlated with expression levels of the reporter gene. The positive control plasmids containing the sGFP ORF expressed sGFP at consistently high levels. However, the co-bombardment experiments, utilizing both strands, did not produce detectable sGFP from R1sGFP. This approach may have also been limited by lack of coordination in timing of

transcription from the DNA expression vectors and/or localization of transcripts in relation to R1sGFP replication within the cell. Furthermore, the TA elements from the DNA vectors were in shorter RNAs than the TA element expressed from pHST2 as a sgRNA. To determine if a shortened RNA length played a role in the lack of *trans*-activation, the TA element was cloned and expressed from a 618 nt TBSV DI-RNA. The DI-TA construct induced sGFP expression from R1sGFP at levels similar to the TA expressed from pHST2 suggesting that a smaller RNA size did not negatively impact *trans*-activation. When comparing helper viruses, the foci produced with the wild type TBSV helper were consistently larger than those with pHST2 as the helper. The negative effect that DI-RNAs have on gene expression in TBSV (Scholthof et al., 1995) was confirmed in these experiments by the reduced rate of movement observed most obviously with pHST2 (which was overcome by the use of RCNMV MP+ *N. benthamiana* with pHST2 co-inoculations). This may be due to the reduced pathogenicity of pHST2 which lacks p19, the TBSV suppressor of gene silencing (Qiu et al., 2002; Qu and Morris, 2002). The success of the DI-RNA experiments suggest that low levels of RNA production from the DNA expression vectors, rather than transcript length, was the cause for lack of detectable sGFP induction in the co-bombardment experiments.

The next approach taken involved mutagenesis of the TA loop nucleotides to produce non Watson-Crick base pairing in a strand specific manner. Mutants M19-M21 contained C→U alterations, while mutant M27 contained a G→A mutation that would result in a potential GU base pair in the negative strand. Despite the potential for 8 base-pairs, containing 1-3 non-canonical pairs for mutants M19-21, only mutant M19

induced detectable sGFP synthesis at 25% of wild-type TA activity. The lack of *trans*-activation by these mutants with GU base pairs suggests that non-canonical interactions between the TA/TABS are not well tolerated. This may be due to the weakened strength of the interaction when GC base pairs with 3 H-bonds are substituted with GU base pairs containing only 2 H-bonds. Conversely, the folded structure of the TA may be altered by the presence of the U residues. Since mutant M27 was unable to induce detectable sGFP expression, we cautiously concluded that the TA/TABS interaction occurs on the positive strands.

To further test our +/+ strand interaction hypothesis from the loop mutation results, additional mutations were made to H1 of the TA element. Mutants M24-M26 were designed to allow GU base pairing and maintenance of H1 in the positive strand while mutants M28-M30 were designed to maintain H1 in the negative strand. Only mutants M24-M26 exhibited detectable sGFP induction from R1sGFP co-inoculations, conclusively proving that the TA/TABS interaction occurred on positive RNA strands. Once again, the presence of non-canonical base pairs reduced the level of sGFP induction suggesting that the TA structure requires a very stable H1 stem.

Once formed, the stability of the TA/TABS complex would be an absolute prerequisite for its proposed function of terminating the RCNMV polymerase complex during minus strand synthesis. This can only be accomplished by the presence of many strong GC base pairs which have been phylogenetically conserved among the dianthoviruses. However, this interaction cannot be so strong as to prevent full-length minus strand synthesis. How does the virus know when to switch from full-length minus strand synthesis to sgRNA template synthesis? Perhaps, the TA/TABS interaction is

merely concentration dependent and is favored only later in the viral replication cycle when both RNAs are at high enough concentrations for the potential interaction to take place. This concept is at least partially supported by the fact that viral or DI replicons are required to generate sufficient TA *in vivo* to *trans*-activate. Strong promoters for gene expression were insufficient to deliver high enough levels of RNA. The loop mutations have shown that the TA/TABS interaction has been finely tuned since most changes affect the level of *trans*-activation. Thus, the TA/TABS interaction as a timing mechanism for sgRNA synthesis awaits further study.

Materials and Methods

Cloning of the RNA-2 TA element

RCNMV RNA-2 TA mutant constructs were generated by annealing complementary mutant oligonucleotides (see Table 2) followed by ligation into *Sna*BI/*Xho*I restricted TBSV vector (pHST2) as in Sit et al. (1998). The wild-type RNA-2 TA element was inserted into the TBSV DI-RNA clone DI-72SXP (Ray and White, 1999). Complementary oligonucleotides [TANsi/Sph/Pst(+) and (-); see Table 3] were annealed and ligated into *Pst*I restricted DI-72SXP to produce constructs DI-TA and DI-TA(-). All constructs were sequenced to verify the presence of the various forms of the TA element.

Construction of transient plant DNA expression vectors

The RCNMV RNA-2 MP ORF (containing the TA element) was cloned in both orientations into the transient plant expression vectors pRTL2 and pE1578. These plasmids contain the enhanced double 35S promoter (Carrington et al., 1990) and the chimeric Super promoter (Ni et al., 1995), respectively. The MP ORF was amplified by the polymerase chain reaction (PCR) from the infectious RCNMV RNA-2 clone (pRC2IG) with oligonucleotide primers RC2 88 *NcoI/EcoRI* and RC2 MP(-)X/M for the positive orientation while the negative orientation was produced with RC2 MP(-) *NcoI/EcoRI* and RC2 XBA/ATG-MP. Both PCR products were digested with *NcoI/XbaI* and ligated into similarly restricted pRTL2 to yield constructs pRTL2-MP(+) and pRTL2-MP(-), respectively. pRTL2-MP(+) was subsequently digested with *EcoRI/XbaI* and ligated into similarly digested pE1578 to yield construct pE1578-MP(+). pRC2IG was restricted with *NheI/MscI* to yield a fragment that was ligated into pE1578 digested with *HincII/XbaI* to generate plasmid pE1578-MP(-).

As an expression control, the sGFP ORF was cloned into both pRTL2 and pE1578 using plasmid sGFP6H.4 as the source of the sGFP ORF. sGFP6H.4 was produced by amplifying the sGFP ORF from plasmid blue-SGFP-TYG-nos KS with oligonucleotide primers sGFP 5' 6X HIS and sGFP 3' MLU/XBA followed by ligation into the pGEM 5Z(+) TA cloning vector. pRTL2-sGFP was produced by digestion of sGFP6H.4 with *NcoI/XbaI* followed by ligation into similarly digested pRTL2 while pE1578-sGFP was produced by digestion of sGFP6H.4 with *PstI/XbaI* followed by ligation into similarly digested pE1578.

Inoculation of *N. benthamiana* with RCNMV, TBSV and mutant transcripts

Infectious RNA transcripts of RCNMV RNAs or TBSV-based constructs were synthesized *in vitro* with T7 RNA polymerase according to Pokrovskaya and Gurevich (1994). 5 µl of each infectious RNA transcript was combined with 100 µl of 10mM sodium phosphate buffer, pH 7.2, then rub-inoculated onto carborundum-dusted *N. benthamiana* leaves. Additional experiments with the TBSV DI-RNA constructs were also performed on RCNMV MP+ transgenic *N. benthamiana* (Vaewhongs and Lommel, 1995) to overcome the reduced level of movement observed with pHST2 as the helper virus. The inoculated plants were placed in a glasshouse at 20-25°C under ambient light conditions. Inoculated leaves were examined for sGFP production 2-3 days post-inoculation (dpi) using a Zeiss Axiophot epifluorescence microscope (Carl Zeiss, Oberkochen, Baden-Wuerttemberg, Germany) equipped with an FITC filter set. Images were acquired with a Leica MZ FLIII fluorescence stereomicroscope equipped with the GFP Plus Fluorescence filter set (Leica Microsystems AG, Wetzlar, Germany) and a Hamamatsu Cooled Color CCD camera. Each inoculation was repeated at least three times.

Co-bombardment of RNA transcripts and DNA expression vectors

For co-bombardment experiments, gold particles (1.5 µg in 25 µl 50% glycerol) were coated with 2.5 µg circular plasmid DNA, 5 µg R1sGFP T7 RNA transcripts, 25 µl 2.5 M CaCl₂, and 10 µl 0.1 M spermidine. DNA expression control bombardments (pRTL2-sGFP and pE1578-sGFP) were prepared as above but without the T7 RNA transcripts. RNA expression control bombardments were prepared without plasmid DNA and included an additional 5 µg of RCNMV RNA-2 T7 RNA transcripts. Detached *N.*

benthamiana leaves were bombarded in a Bio-Rad PDS-1000/He unit at 1100 p.s.i. with a sample distance of 9 cm. Bombarded leaves were incubated for 24-48 hrs at room temperature in petri dishes with moistened paper toweling. Leaves were examined for sGFP expression as mentioned above, 24-48 hrs post-bombardment.

Acknowledgments

We thank J. Sheen for the GFP plasmid, H. Scholthof for the pHST2 vector, A. White for the DI72-SXP construct, J. Carrington for the pRTL2 vector and S. Gelvin for the pE1578 vector. This research was supported by USDA NRI grant 98-02298 and NSF grant MCB-0077964 to S.A.L. and T.L.S.

References

- Carrington, J.C., Freed, D.D., Oh, C-S., 1990. Expression of potyviral polyproteins in transgenic plants reveals three proteolytic activities required for complete processing. *EMBO J* 9, 1347-1353.
- Choi, I.-R., Ostrovsky, M., Zhang, G., White K.A., 2001. Regulatory activity of distal and core RNA elements in Tombusvirus subgenomic mRNA2 transcription. *J Biol Chem* 276, 41761-41768.
- Choi, I.-R., White, K.A., 2002. An RNA activator of subgenomic mRNA1 transcription in tomato bushy stunt virus. *J Biol Chem* 277, 3760-3766.

- Eckerle, L.D., Ball, L.A., 2002. Replication of the RNA segments of a bipartite viral genome is coordinated by a transactivating subgenomic RNA. *Virology* 296, 166-176.
- Eckerle, L.D., Albarino, C.G., Ball, L.A., 2003. *Flock House virus* subgenomic RNA3 is replicated and its replication correlates with transactivation of RNA2. *Virology* 317, 95-108.
- Kim, K.-H., Hemenway, C.L., 1999. Long-distance RNA-RNA interactions and conserved sequence elements affect potato virus X plus-strand RNA accumulation. *RNA* 5, 636-645.
- Kim, K.H., Lommel, S.A., 1994. Identification and analysis of the site of -1 ribosomal frameshifting in red clover necrotic mosaic virus. *Virology* 200, 574-582.
- Kim, K.-H., Lommel, S.A., 1998. Sequence element required for efficient -1 ribosomal frameshifting in red clover necrotic mosaic dianthovirus. *Virology* 250, 50-59.
- Lindenbach, B.D., Sgro, J.-Y., Ahlquist, P., 2002. Long-distance base pairing in flock house virus RNA1 regulates subgenomic RNA3 synthesis and RNA2 replication. *J Virol* 76, 3905-3919.
- Lommel, S.A., Weston-Fina, M., Xiong, Z., Lomonossoff, G.P., 1988. The nucleotide sequence and gene organization of red clover necrotic mosaic virus RNA-2. *Nucleic Acids Res* 16, 8587-8602.
- Miller, W.A., Koev, G., 2000. Synthesis of subgenomic RNAs by positive-strand RNA viruses. *Virology* 273, 1-8.

- Ni, M., Cui, D., Einstein, J., Narasimhulu, S., Vergara, C.E., Gelvin, S.B., 1995. Strength and tissue specificity of chimeric promoters derived from the octopine and mannopine synthase genes. *Plant J* 7, 661-676.
- Okuno, T., Hiruki, C., Rao, D.V., Figueiredo, G.C., 1983. Genetic determinants distributed in two genomic RNAs of sweet clover necrotic mosaic, red clover necrotic mosaic and clover primary leaf necrosis viruses. *J Gen Virol* 64, 1907-1914.
- Osman, T.A.M., Buck, K.W., 1987. Replication of red clover necrotic mosaic virus RNA in cowpea protoplasts: RNA-1 replicates independently of RNA-2. *J Gen Virol* 68, 289-296.
- Pokrovskaya, I.D., Gurevich, V.V., 1994. *In vitro* transcription: preparative RNA yields in analytical scale reactions. *Anal Biochem* 220, 420-423.
- Qiu, W., Park, J.-W., Scholthof, H.B., 2002. Tombusvirus P19-mediated suppression of virus-induced gene silencing is controlled by genetic and dosage features that influence pathogenicity. *MPMI* 15, 269-280.
- Qu, F., Morris, T.J., 2002. Efficient infection of *Nicotiana benthamiana* by tomato bushy stunt virus is facilitated by the coat protein and maintained by p19 through suppression of gene silencing. *MPMI* 15, 193-202.
- Ray, D., White, K.A., 1999. Enhancer-like properties of an RNA element that modulates tombusvirus RNA accumulation. *Virology* 256, 162-171.
- Sit, T.L., Vaewhongs, A.A., Lommel, S.A., 1998. RNA-mediated trans-activation of transcription from a viral RNA. *Science* 281, 829-832.

- Vaewhongs, A.A., Lommel, S.A., 1995. Virion formation is required for the long-distance movement of red clover necrotic mosaic virus in movement protein transgenic plants. *Virology* 212, 607-613.
- White, K.A., 2002. The premature termination model: a possible third mechanism for subgenomic mRNA transcription in (+)-strand RNA viruses. *Virology* 304, 147-154.
- Xiong, Z., Lommel, S.A., 1989. The complete nucleotide sequence and genome organization of red clover necrotic mosaic virus RNA-1. *Virology* 171, 543-554.
- Xiong, Z., Kim, K.H., Giesman-Cookmeyer, D., Lommel, S.A., 1993a. The roles of the red clover necrotic mosaic virus capsid and cell-to-cell movement proteins in systemic infection. *Virology* 192, 27-32.
- Xiong, Z., Kim, K.H., Kendall, T.L., Lommel, S.A., 1993b. Synthesis of the putative red clover necrotic mosaic virus RNA polymerase by ribosomal frameshifting *in vitro*. *Virology* 193, 213-221.
- Zavriev, S.K., Hickey, C.M., Lommel, S.A., 1996. Mapping of the red clover necrotic mosaic virus subgenomic RNA. *Virology* 216, 407-410.
- Zhang, G., Slowinski, V., White, K.A., 1999. Subgenomic mRNA regulation by a distal RNA element in a (+)-strand RNA virus. *RNA* 5, 550-561.
- Zhong, W., Rueckert, R.R., 1993. Flock house virus: down-regulation of subgenomic RNA3 synthesis does not involve coat protein and is targeted to synthesis of its positive strand. *J Virol* 67, 2716-2722.
- Zuker, M., 2003. Mfold web server for nucleic acid folding and hybridization prediction. *Nucleic Acids Res* 31, 3406-3415.

TABLE 1

Accumulation of sGFP after co-bombardment of *Nicotiana benthamiana* leaves with R1sGFP transcripts and DNA constructs expressing the TA element

| DNA Inoculum | RNA Inoculum | sGFP Expression |
|---------------------|---------------------|------------------------|
| pRTL2-MP(+) | R1sGFP | - |
| pRTL2-MP(-) | R1sGFP | - |
| pRTL2-sGFP | - | + |
| pE1578-MP(+) | R1sGFP | - |
| pE1578-MP(-) | R1sGFP | - |
| pE1578-sGFP | - | + |
| - | R1sGFP + RC2 | + |

TABLE 2
Oligonucleotides for Cloning/PCR

| Oligonucleotide | Sequence |
|-----------------|---|
| TA-WT | GTATCGATCAATCAGAGGTATCGCCCCGCCTCTCAGTGTTGC |
| TA MUT | GTATCGATCAATCAGAGGTAaCGgCCgGCCTCTCAGTGTTGC |
| M1 | GTATCGATCAATCAGAGGTAaCGCCCCGCCTCTCAGTGTTGC |
| M2 | GTATCGATCAATCAGAGGTATCGgCCCGCCTCTCAGTGTTGC |
| M3 | GTATCGATCAATCAGAGGTATCGCCCgGCCTCTCAGTGTTGC |
| M4 | GTATCGATCAATCAGAGGTAaCGgCCCGCCTCTCAGTGTTGC |
| M5 | GTATCGATCAATCAGAGGTAaCGCCCgGCCTCTCAGTGTTGC |
| M6 | GTATCGATCAATCAGAGGTATCGgCCgGCCTCTCAGTGTTGC |
| M7 | GTATCGATCAATCAGAGGTATCGCCCCGCCTCT--G-GTTGC |
| M8 | GTATCGATCAATCgcctctATCGCCCCagagggtCAGTGTTGC |
| M9 | GTATCGATCAATCtctccgATCGCCCCtggagaCAGTGTTGC |
| M10 | GTATCGATCAATcagtA GAGGTATCGCCCCGCCTCTcGTTGC |
| M11 | GTATCGATCAATCtctGGTATCGCCCCGCCagaCAGTGTTGC |
| M12 | GTATCGATCAATCAGaccgATCGCCCCtggTCTCAGTGTTGC |
| M13 | GTATCGATCAATCAGAGGcATCGCCCCGCCTCTCAGTGTTGC |
| M14 | GTATCGATCAATCAGAGGTgaCGCCCCGCCTCTCAGTGTTGC |
| M15 | GTATCGATCAATCAGAGGTtaCGCCCCGCCTCTCAGTGTTGC |
| M16 | GTATCGATCAATCAGAGGTtagGCCCGCCTCTCAGTGTTGC |
| M17 | GTATCGATCAATCAGAGGTtagcCCCCGCCTCTCAGTGTTGC |
| M18 | GTATCGATCAATCAGAGGTtagcgCCCGCCTCTCAGTGTTGC |
| M19 | GTATCGATCAATCAGAGGTATtGCCCGCCTCTCAGTGTTGC |
| M20 | GTATCGATCAATCAGAGGTATtGtCCCGCCTCTCAGTGTTGC |
| M21 | GTATCGATCAATCAGAGGTATtGttCCCGCCTCTCAGTGTTGC |
| M22 | GTATCGATCAATCAGAGGTATCGCCCCaCCTCTCAGTGTTGC |
| M23 | GTATCGATCAATCAGAGGgatCGCCCCtCCTCTCAGTGTTGC |
| M24 | GTATCGATCAATCAGAGGTATCGCCCCGcttTCAGTGTTGC |
| M25 | GTATCGATCAATCAGAGGTATCGCCCCGctTCTCAGTGTTGC |
| M26 | GTATCGATCAATCAGAGGTATCGCCCCGCCTtTCAGTGTTGC |
| M27 | GTATCGATCAATCAGAGGTATCaCCCCGCCTCTCAGTGTTGC |
| M28 | GTATCGATCAATCAGAAgTATCGCCCCGCCTCTCAGTGTTGC |
| M29 | GTATCGATCAATCAaAGGTATCGCCCCGCCTCTCAGTGTTGC |
| M30 | GTATCGATCAATCAaAaGTATCGCCCCGCCTCTCAGTGTTGC |

| | |
|--------------------------|--|
| TANsi/Sph/Pst(+) | TGCAATCAGAGGTATCGCCCCGCCTCTCAGTGTTGCTGCA |
| TANsi/Sph/Pst(-) | GCAACACTGAGAGGCGGGGCGATACCTCTGATTGCATGCA |
| RC2 88 <i>NcoI/EcoRI</i> | GTAACCATGGCTGAATTCATGTGGAAAATTTAAGTG |
| RC2 MP(-)X/M | GTACGCGTCTAGAGTCTTTCCGGATTTGG |
| RC2 MP(-)NcoI/EcoRI | GTAACCATGGAATTCTAGAGTCTTTCCGGATTTGG |
| RC2 XBA/ATG-MP | GTAATCTAGATGGCTGTTTCATGTGG |
| sGFP 5' 6X HIS | GTCCATGGGATCGATG(CAT) ₆ GTGAGCAAGGGCGAGGAGCTG |
| sGFP 3' MLU/XBA | GCTCTAGACGCGTTACTTGTACAGCTCGTCC |

Only (+) strand oligonucleotides are shown for TA-WT, TA-MUT and M1-M30. Altered nucleotides are indicated in lower case with the exception of M7 where deleted sequences are shown as hyphens. The underlined sequence in TA-WT represents a diagnostic *Clal* site also present in TA-MUT and M1-M30 oligonucleotides.

Figure Legends

Fig. 1. Genome organization of *Red clover necrotic mosaic virus* (RCNMV) viral RNAs.

A) RCNMV RNAs 1 and 2 are depicted. A comparison of dianthoviral RNA-1 sequences around the *trans*-activator binding sequence (TABS; boxed nucleotides) is shown below RNA-1. SCNMV, *Sweet clover necrotic mosaic virus*; CRSV, *Carnation ringspot virus*.

Shaded TABS nucleotides are complementary to the *trans*-activator (TA) loop sequence. The location of the TA element (depicted as a stem-loop structure) on RNA-2 is indicated. B) R1sGFP. The RNA-1 sGFP reporter construct is depicted. The TABS of R1sGFP and the R1sGFP mutant (R1sGFP-M) are shown below the genome map. The amino acid sequence for p88 is shown above the sequence in single letter code. The Glu→Asp mutation in R1sGFP-M is indicated by E/D. Shaded nucleotides represent alterations from the wild-type sequence. C) *Tomato bushy stunt virus* (TBSV) constructs. Wild-type TBSV, and the TBSV vector, pHST2, without and with an insert (TA-Mn) are depicted. Boxes represent specific open reading frames with names of encoded proteins within. Right-angle arrow indicates subgenomic RNA transcription start site. Stem-loop in TA-Mn indicates mutant TA element inserted into the TBSV genome. (- FS) indicates -1 ribosomal frameshift. UAG indicates amber readthrough termination codon.

Fig. 2. Covariant RCNMV RNA-2 TA loop mutants. Various TA loop mutant constructs were cloned and expressed from the TBSV vector pHST2. Mutated nucleotides are denoted with open typeface. Non-complementary nucleotides are depicted in open typeface with a black background. TA mutant constructs M1-M6 were co-inoculated with

either R1sGFP or R1sGFP-M (TABS sequences are depicted below respective headings) and examined 2-3 days post-inoculation for sGFP expression. sGFP expression levels relative to wild-type TA for R1sGFP or TA MUT for R1sGFP-M: +++, 100%; +/-, <10%; -, not detected.

Fig. 3. Sample fluorescence dissecting scope images of sGFP expression from R1sGFP induced by co-inoculated pHST2-TA-Mn constructs. Inoculated *N. benthamiana* leaves were examined 2-3 days post-inoculation. A) TA-WT. B) TA-M1. C) TA-M3. D) TA-M6. Bar in panel D equals 10 μ m.

Fig. 4. Minimal binding and strand specific TA loop mutants. Altered nucleotides are denoted with open typeface. Non-complementary nucleotides are depicted in open typeface with a black background. TA mutant construct transcripts were co-inoculated with R1sGFP (TABS sequences are depicted below respective headings) and examined 2-3 days post-inoculation for sGFP expression. sGFP expression relative to wild-type TA: +++, 100%; ++, 50%; +, 25%; -, not detected.

Fig. 5. Structural and strand specific TA stem mutants. Mutated nucleotides are denoted with open typeface. Mutations are arranged according to the TA feature mutated as noted above each grouping. TA mutant construct transcripts were co-inoculated with R1sGFP and examined 2-3 days post-inoculation for sGFP expression. sGFP expression relative to wild-type TA: +++, 100%; ++, 50%; +, 25%; +/-, <10%; -, not detected.

Fig. 6. Effect of TBSV helper virus on sGFP expression from R1sGFP induced by DI-TA construct. Inoculated leaves were examined 3 days post-inoculation. A) pHST2 helper with DI-TA. B) TBSV wild-type helper with DI-TA. C) Wild-type RCNMV RNA-2 without DI-TA. Bar in panel C represents 200 μm .

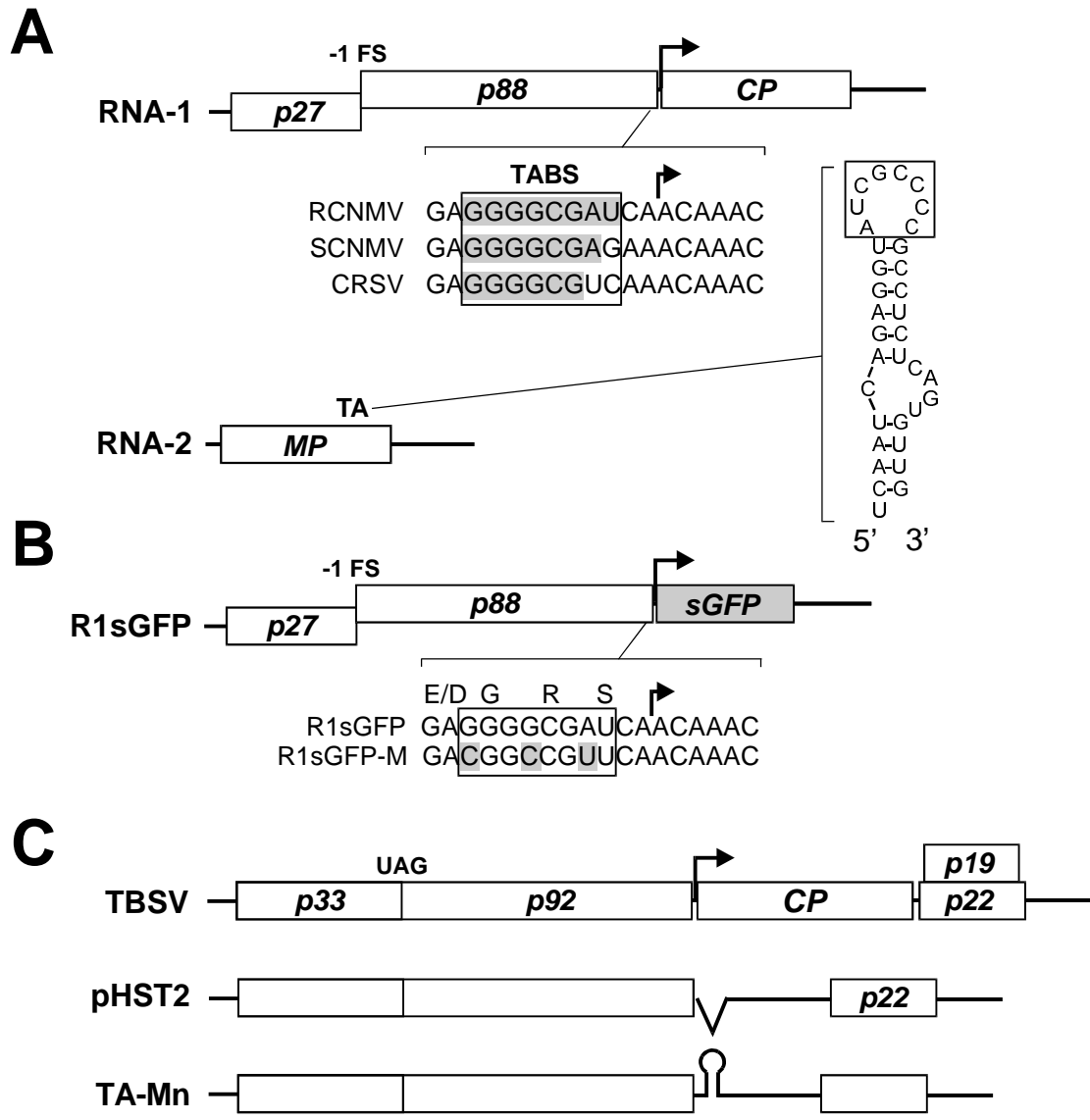


Fig. 1

| TA Clone | | Complementarity to R1sGFP 3' UAGCGGGG 5' | sGFP | Complementarity to R1sGFP-M 3' UUGCCGGC 5' | sGFP |
|----------|--|--|------|--|------|
| WT | | 5' AUCGCCCC 3' | +++ | 5' AUCGCCCC 3' | - |
| MUT | | AACGGCCG | - | AACGGCCG | +++ |
| M1 | | AACGCCCC | +++ | AACGCCCG | - |
| M2 | | AUCGCCCG | - | AUCGGCCG | +/- |
| M3 | | AUCGCCCG | +/- | AUCGCCCG | - |
| M4 | | AACGGCCC | - | AACGGCCG | - |
| M5 | | AACGCCCG | +/- | AACGCCCG | - |
| M6 | | AUCGCCCG | - | AUCGGCCG | +/- |

Fig. 2

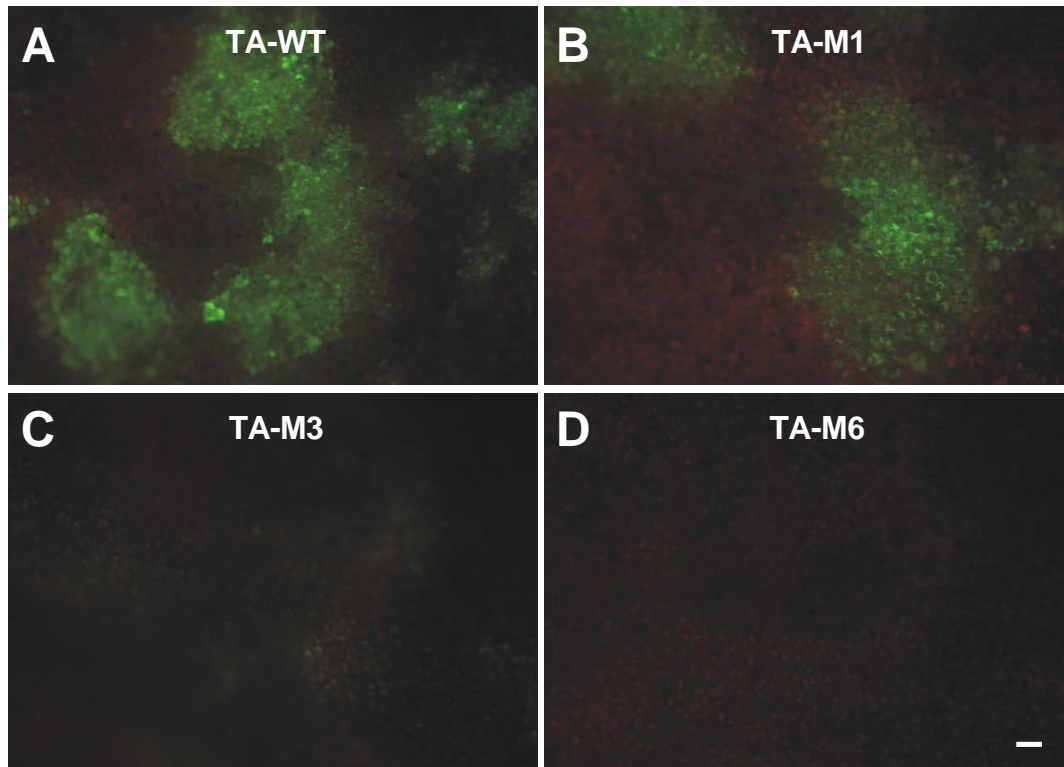


Fig. 3

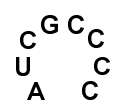
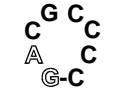
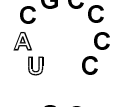
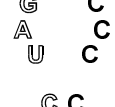
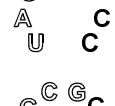
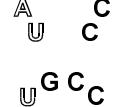
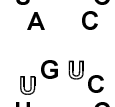
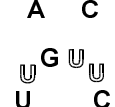
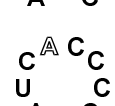

| TA Clone | Complementarity to R1sGFP | | sGFP |
|----------|---|-----------------------------------|------|
| | (+) strands 3' UAGCGGGG 5' | (-) strands 5' 3' CCCC GCUA 5' | |
| WT |  | 5' AUCGCCCC 3' 5' GGGGCGAU 3' | +++ |
| M14 |  | GACGCCCC GGGGCGUC | + |
| M15 |  | UACGCCCC GGGGCGUA | ++ |
| M16 |  | UAGGCCCC GGGGCCUA | - |
| M17 |  | UAGC CCCC GGGG GCUA | - |
| M18 |  | UAGCG CCC GGG CGCUA | - |
| M19 |  | AUUGCCCC GGGGC AU | + |
| M20 |  | AUUGUCCC GGG ACAU | - |
| M21 |  | AUUGUUCC GG AACAU | - |
| M27 |  | AUCACCCC GGGGUGAU | - |

Fig. 4

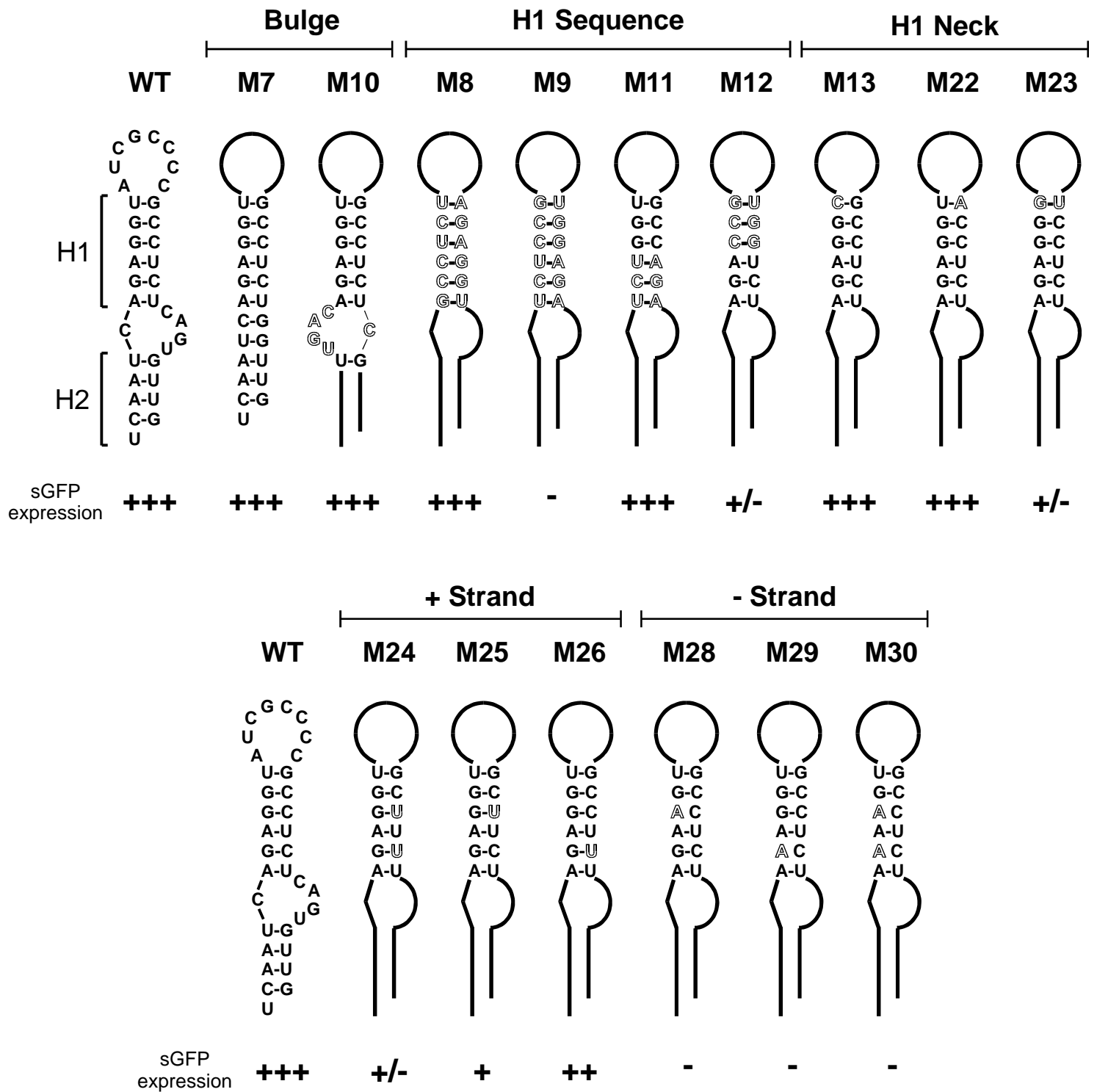


Fig. 5

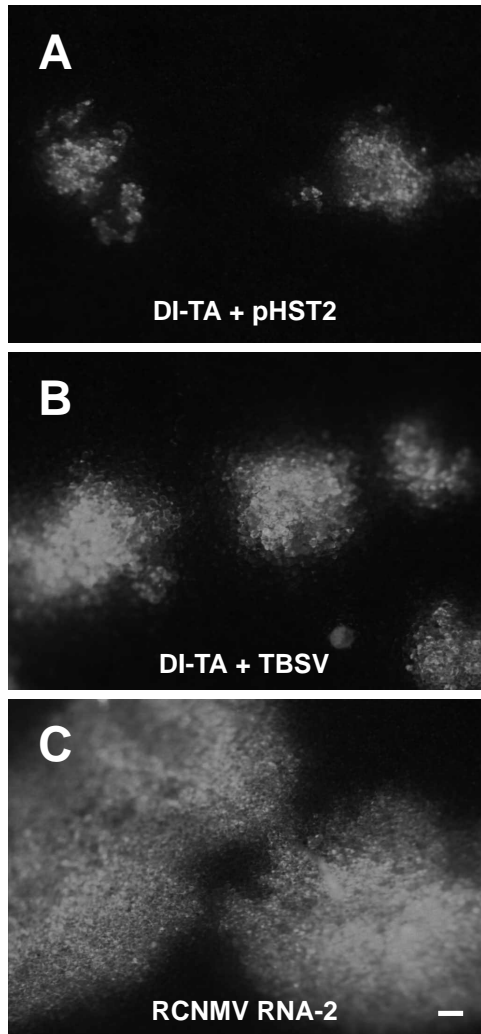


Fig. 6